Journal of Chromatography A 1673 (2022) 463071

Contents lists available at ScienceDirect

Journal of Chromatography A

journal homepage: www.elsevier.com/locate/chroma

Hydroxyl-functionalized three-dimensional covalent organic framework for selective and rapid extraction of organophosphorus pesticides

Mei-Lan Du[a,b,c], Cheng Yang[a,b,c], Hai-Long Qian[a,b,c,*], Xiu-Ping Yan[a,b,c,d,*]

[a] State Key Laboratory of Food Science and Technology, Jiangnan University, Wuxi 214122, China
[b] International Joint Laboratory on Food Safety, Jiangnan University, Wuxi 214122, China
[c] Institute of Analytical Food Safety, School of Food Science and Technology, Jiangnan University, Wuxi 214122, China
[d] Key Laboratory of Synthetic and Biological Colloids, Ministry of Education, Jiangnan University, Wuxi 214122, China

ARTICLE INFO

Article history:
Received 1 April 2022
Revised 12 April 2022
Accepted 14 April 2022
Available online 16 April 2022

Keywords:
Three-dimensional covalent organic framework
Adsorbent
Dispersed-solid phase extraction
Organophosphorus pesticides

ABSTRACT

The wide utilization of organophosphorus pesticides (OPPs) results in a potential threat to ecosystem and human health. The essential extraction process in practical OPPs analysis always suffers from the low efficiency due to the limited accessible active sites and interactions in the adsorbents. Here, we report a rational design and synthesis of a novel hydroxyl-functionalized three-dimensional covalent organic framework (3D COF-OH) named JNU-6 with ordered porous structure and multiple interactions as the adsorbent for rapid and selective dispersive solid phase extraction (DSPE) of OPPs. The 3D COF-OH based DSPE was coupled with gas chromatography-flame thermionic detection (GC-FTD) for the determination of four selected OPPs with low limits of detection of 0.15–0.39 ng mL^{-1}, wide linear range of 1–1100 ng mL^{-1}. The developed method gave good precision (relative standard deviation of 1.6–8.5% ($n = 5$)) and recoveries of 86–106% for the determination of OPPs in complicated fruit and vegetable samples. This work reveals the high practical potential of functionalized 3D COFs as adsorbents for effective extraction of trace contaminants in complicated samples.

1. Introduction

Pesticides have shown the irreplaceability for modern agriculture. The wide utilization of organophosphorus pesticides (OPPs) results in their severe residue in the soil, water and food, increasing the potential threat to ecosystem and human health [1–4]. The high inhabitation of trace OPPs to the cholinesterase of organisms leads to the injury of nervous leptin and respiratory system or even death [5–7]. Therefore, many governments and regions including China, USA, European Union (EU) and Codex Alimentarius Commission have established stringent regulations of OPPs to ensure food safety [8,9]. For example, the EU limits the maximum allowable level of 0.05 mg kg^{-1} for parathion in grape [10]. In this regard, advanced analytical methods are required for OPPs to ensure the smooth implementation of the regulations.

Selective extraction is essential for the precise determination of OPPs residue due to the trace level of OPPs and severe interference of complex sample matrix [11]. However, the validated commercial adsorbent of Sep-PakNH_2 (amino functionalized silica) for the extraction of OPPs suffers from time-consuming and low anti-interference [12]. Therefore, novel materials such as carbon materials [13,14], molecularly imprinted polymers [15–17], and metal-organic frameworks [18–20] have been developed as the adsorbents to promote the extraction of OPPs over the past few decades. In most of previous sorbents, hydrophobic interactions, hydrogen bonds, and π-π interactions were explored as driving forces for the extraction of OPPs. Even so, an adsorbent with great stability, high selectivity and rapid kinetics is still realistically preferred, but remains challenging.

Covalent organic frameworks (COFs) are emerging crystalline polymers consisting of organic monomer with strong covalent bonds, and draw great concern owing to their remarkable applications in diverse areas [21–24]. The stable and ordered structure with large surface area endows COFs with high practical ability as adsorbents for selective and rapid interaction with the analytes [25,26]. To date, two-dimensional (2D) COFs are widely applied in the extraction of contaminants [27,28]. In comparison with 2D COFs, 3D COFs can offer more complicate pores to promote the accessibility of analytes [29,30]. Therefore, the application of

* Corresponding authors at: State Key Laboratory of Food Science and Technology, Jiangnan University, Wuxi 214122, China.
E-mail addresses: hlqian@jiangnan.edu.cn (H.-L. Qian), xpyan@jiangnan.edu.cn (X.-P. Yan).

https://doi.org/10.1016/j.chroma.2022.463071
0021-9673/

3D COFs for selective and rapid extraction of OPPs is of great promise.

Herein, we show rational design and synthesis of a hydroxyl-functionalized 3D COF (3D COF-OH) named as JNU-6 as efficient adsorbent for rapid and selective extraction of trace OPPs. Tetra (4-aminophenyl) methane (TAM) with symmetrical tetrahedral structure and rich hydroxyl group-containing 2,6-dihydroxynaphthalene-1,5-dicarbaldehyde (DHNDA) are chosen as the building monomers to construct JNU-6. The obtained crystalline structure, large surface area and great stability of JNU-6 are beneficial for the rapid extraction of OPPs. The rich aromatic ring and hydroxyl group of JNU-6 further offer multiple hydrophobic interaction, hydrogen bonding interaction, and π-π interaction to promote the selectivity to OPPs. The JNU-6-based dispersive solid phase extraction (DSPE) coupled to gas chromatography with flame thermionic detector (GC-FTD) shows promising for the determination of OPPs in real fruit and vegetable samples. This work reveals the high potential of 3D COFs as the adsorbent for rapid and selective extraction of trace contaminants.

2. Materials and methods

2.1. Reagents

All the reagents used in the experiment were at least analytical grade. Ultrapure water was obtained from Wahaha Foods Co., Ltd. (Hangzhou, China). TAM and DHNDA were purchased from Jilin Chinese Academy of Sciences-Yanshen Technology Co., Ltd. (Jilin, China). Acetonitrile (ACN), Methanol (MeOH), tetrahydrofuran (THF), isopropanol (IPA), o-dichlorobenzene (o-DCB), N-butyl alcohol (BuOH), ethyl acetate (EA), n-hexane, mesitylene, acetic acid, 1,4-dioxane, ammonium hydroxide, sodium hydroxide (NaOH), hydrochloric acid (HCl) were purchased from Shanghai Sinopharm Chemical Reagent Co., Ltd (Shanghai, China). A certified reference material MRM0666 (apple juice) were from Meizheng Group (Beijing, China). The standard solution of parathion methyl (PAM), parathion (PA), profenofos (PFF) and phosalone (PHO) were purchased from Aladdin Chemistry Co., Ltd. (Shanghai, China). The mixed stock solution of 100 μg mL^{-1} was prepared with acetonitrile and stored at −18 °C. The standard solution of 1 μg mL^{-1} was prepared by step-by-step dilution of the stock solution with acetonitrile.

2.2. Synthesis of JNU-6

Typically, TAM (0.09 mmol, 34.2 mg) and DHNDA (0.18 mmol, 38.9 mg) were mixed with 12 M acetic acid (0.9 mL) and 1,4-dioxane (0.1 mL) in a 35 mL pressure-proof tube (OD 26 × L 125 mm). After 15 min sonication, the mixture was degassed with three freeze–pump–thaw cycles, and then reacted at 120 °C for 3 days. The obtained precipitate was collected by centrifugation, washed with THF and H_2O for three times, and extracted with THF. Finally, the red powder was dried under vacuum at 70 °C for 24 h to give 3D COF JNU-6 with 75% yield.

2.3. Instrumentation

Powder X-ray diffractometer (PXRD) patterns were recorded on a D2 Phaser X-ray diffractometer (Bruker AXS GmbH, Germany) with a scanning speed of 8° min^{-1} and a step size of 0.05° in 2θ. Fourier transform infrared (FTIR) spectra were obtained from IS20 FTIR spectrometer (Nicolet, USA). Thermogravimetric analysis (TGA) was performed on a thermogravimetric analyzer (PTC-10A, Rigaku, Japan) from 25 to 800 °C in flowing nitrogen at a heating rate of 10 °C min^{-1}. ^{13}C solid-state nuclear magnetic resonance (^{13}C SNMR) spectra were recorded on AVANCE III HD 400 MHz (Bruker, Germany). Scanning electron microscope (SEM) images were recorded on a su1510 scanning electron microscope (Rigaku, Japan). Transmission electron microscopy (TEM) images were obtained on a JEM-2100 transmission electron microscope (Rigaku, Japan). Nitrogen adsorption-desorption experiments were performed on a nitrogen adsorption analyzer with a 77 K nitrogen adsorption (Autosorb-IQ, Quantachrome, USA).

Identification and quantification of target analytes were performed on a GC-2030 system with FTD detector (Shimadzu, Japan) and an HP-5 commercial capillary column (30 m × 0.32 mm × 0.25 μm). Nitrogen was used as the carrier gas at the constant flow rate of 2.0 mL min^{-1} and injection volume was 1.0 μL. Injector temperature was 220 °C, and the detector temperature was 290 °C. The oven temperature was programed as follows: 60 °C held for 1 min, and then the temperature was increased to 220 °C at 40 °C min^{-1} and hold for 2 min. Finally, the temperature was raised to 290 °C at 45 °C min^{-1} and maintained for 3 min.

2.4. Sample preparation

Briefly, the samples of tomato, cabbage and apple were purchased from the local supermarket. The edible part of the above samples was cut into pieces and homogenized. 2.5 g of the homogenized samples was ultrasonically extracted with 10 × 2 mL ACN for 20 min. The supernatant of each extraction was collected by centrifugation at 9000 rpm for 8 min. Finally, the obtained supernatant was dried on termovap sample concentrator (N-EVAPTM^{111}, Organomation Associates, Jnc), and redissolved with 1.0 mL ACN as sample solution for further use.

2.5. DSPE procedure

Typically, 1.0 mL above-obtained sample solution was diluted with the acetic acid aqueous solution (pH 6) to 5 mL as the working solution for DSPE. Then, 8 mg JNU-6 was mixed with 5 mL of the working solution. The mixture was shaken on HS501 digital shaker (IKA, Germany) at 180 rpm for 5 min. The JNU-6 was collected by centrifugation at 8500 rpm for 6 min, washed with 0.25 mL ACN twice, and filtered with a 0.22 μm membrane. The filtrate was analyzed by GC-FTD.

3. Results and discussion

3.1. Design and preparation of JNU-6

As selective enrichment of OPPs have been realized with the introduction of hydrophobic interaction, hydrogen bonds, or π-π interaction in previous works [31,32], we selected TAM with symmetrical tetrahedral structure and hydroxyl group-containing DHNDA as the building monomers to prepare JNU-6 (Fig. 1). The symmetrical tetrahedral structure of TAM along with the linear planar structure of DHNDA can guide the formation of hydrophobic 3D structure with large π electron system to offer the π-π interaction and hydrophobic interaction with OPPs. The abundant hydroxyl groups from DHNDA further bring JNU-6 hydrogen bonding interaction to promote the selectivity to OPPs.

Solvent composition, time and temperature for the reaction of TAM and DHNDA were studied in detail to prepare crystalline JNU-6 (Figs. S1–S4). Six different solvent systems were tested for the preparation of JNU-6, and the result showed that 12 M acetic acid/1,4-dioxane was beneficial for the formation of crystalline structure (Fig. S1) due to the appropriate solubility of the monomers in this solvent. Subsequently, the ratio of 12 M acetic acid/1,4-dioxane was further investigated to obtain the optimal reaction rate for the condensation of TAM and DHNDA. The high

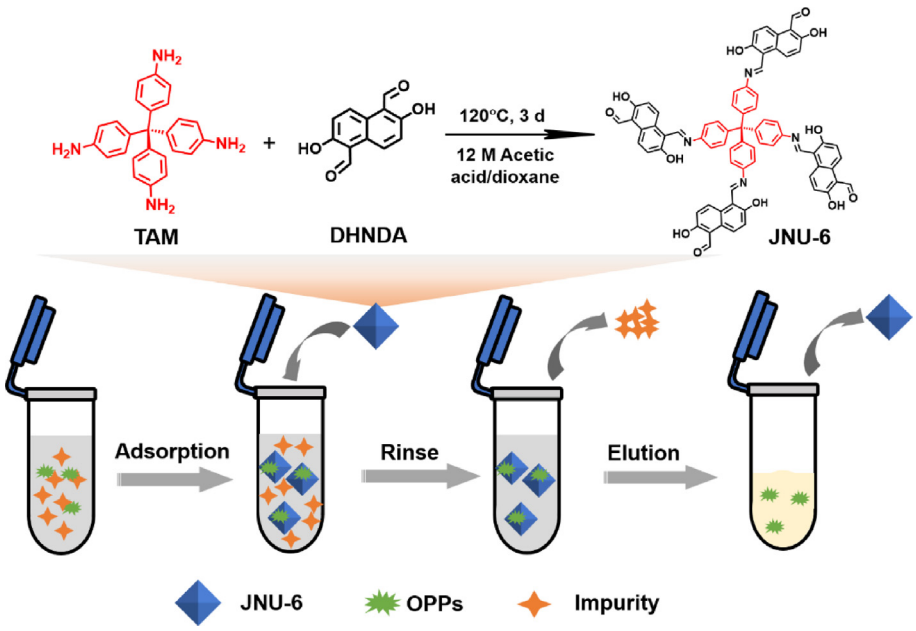

Fig. 1. Schematic for the design of JNU-6 and the process of the JNU-6 based DSPE for OPPs.

crystallinity of JNU-6 identified the preferred v/v ratio of 12 M acetic acid/1,4-dioxane was 9:1 (Fig. S2). The PXRD patterns show that 3 days were needed to give the amorphous polymer to the crystalline structure is time-consuming (Fig. S3).

The crystallinity of JNU-6 was improved as temperature increased (Fig. S4), indicating the indispensability of temperature for the thermodynamic controlling condensation of TAM and DHNDA to give crystalline COF. As a result, 120 °C was chosen for the follow-up experiment because further increase of the temperature gave no obvious promotion of the crystallinity for JNU-6.

3.2. Characterization of JNU-6

The FTIR spectrum of JNU-6 shows a strong characteristic absorption peak at 1618 cm^{-1} for the stretching vibration of C=N bonds, indicating the formation of the imine linkage, while the peak at 3600 cm^{-1} for O-H verifies the introduction of hydroxyl group in JNU-6 (Fig. 2a). The carbon peaks at 160 and 155 ppm in the ^{13}C SNMR spectra of JNU-6 further offer the complementary evidence of imine and hydroxyl group in JNU-6 (Fig. S5).

JNU-6 gave obvious characteristic PXRD peaks at 7.63°, 15.39°, 20.80° and 22.88° (Fig. 2b), indicating its crystalline structure. To figure out the specific structure of JNU-6, the feasible structure was simulated with 3,5,7-fold-interpenetrated diamond net (dia-3, 5 and 7) and the corresponding simulated PXRD patterns were also produced. The experimental PXRD pattern showed the best agreement with the simulated one from dia-5, indicating the structure of JNU-6 was adopted with the dia-5 (Fig. 2b and c). Further refinement gave a more specific dia-5 structure (Rp = 4.81%, ωRp = 6.10%) with unit cell parameters of space group I41/A, $a = b = 23.1373$ Å, $c = 13.6680$ Å, and $\alpha = \beta = \gamma = 90°$ (Fig. 3 and Table S1).

The Brunauer–Emmett–Teller (BET) surface areas, pore volume and pore size of JNU-6 were calculated to be 633.13 $m^2\ g^{-1}$, 1.38 $cm^3\ g^{-1}$, and 10.5 Å, respectively, based on the nitrogen adsorption-desorption isotherm at 77 K (Figs. 2d and S6, S7). The large BET surface area along with porous structure rendered JNU-6 sufficient active sites and good accessibility to interact with the analytes. SEM and TEM images show the aggregated rod-like morphology of JNU-6 (Fig. 2e and f), which is also beneficial for adsorption.

The stability of JNU-6, which is crucial for its application as adsorbent, was further investigated by monitoring the PXRD pattern and FTIR spectra of JNU-6 after soaking in various solutions including ACN, THF, H_2O, 0.1 M HCl and 0.1 M NaOH. The results showed no obvious change of the crystallinity and structure of JNU-6, confirming the high chemical stability of JNU-6 (Figs. S8, S9). The TGA curve further indicates the high thermal stability of JNU-6 up to 420 °C (Fig. S10). The great stability of JNU-6 ensured the availability of JNU-6 as adsorbent for complex samples in harsh conditions.

3.3. Optimization of DSPE

The structures of four OPPs are shown in Table S2. To access the best extraction performance for OPPs, the amount of adsorbent (4–12 mg), extraction time (1–30 min) and solution pH (4–9) were optimized in 40 ng mL^{-1} OPPs. The recovery of the OPPs first increased with the amount of JNU-6 up to 8 mg, then unchanged in the range of 8–12 mg (Fig. 4a). It was found that 5 min was sufficient for the extraction of the OPPs (Fig. 4b). Such fast kinetics for JNU-6 to extract the OPPs could be attributed to the benefit of the ordered structure with large BET area of JNU-6 for the interaction with the OPPs. The effect of pH on the recovery shows the extraction was favorable at pH 6 (Fig. 4c). Further increase of pH over 6 led to the decrease of the recovery of OPPs due to the instability of OPPs in alkali condition. Additionally, the investigation of eluent, elution time and eluent volume demonstrated the application of 2 × 0.25 mL ACN for 6 min was efficient for the elution of the OPPs from JNU-6 (Fig. 4d–f).

3.4. Analytical figures of merit

The obtained optimal extraction and elution conditions were applied for the development of a 3D COF based DSPE-GC-FTD method to determine the four OPPs. The analytical performance of the developed method was evaluated in OPPs spiked aqueous solution (1–1300 ng mL^{-1}) (Fig. S11). The linear relationship between the concentration of OPPs and the peak areas were achieved in a wide range of 1–1100 ng mL^{-1} ($R^2 > 0.9966$). The detection lim-

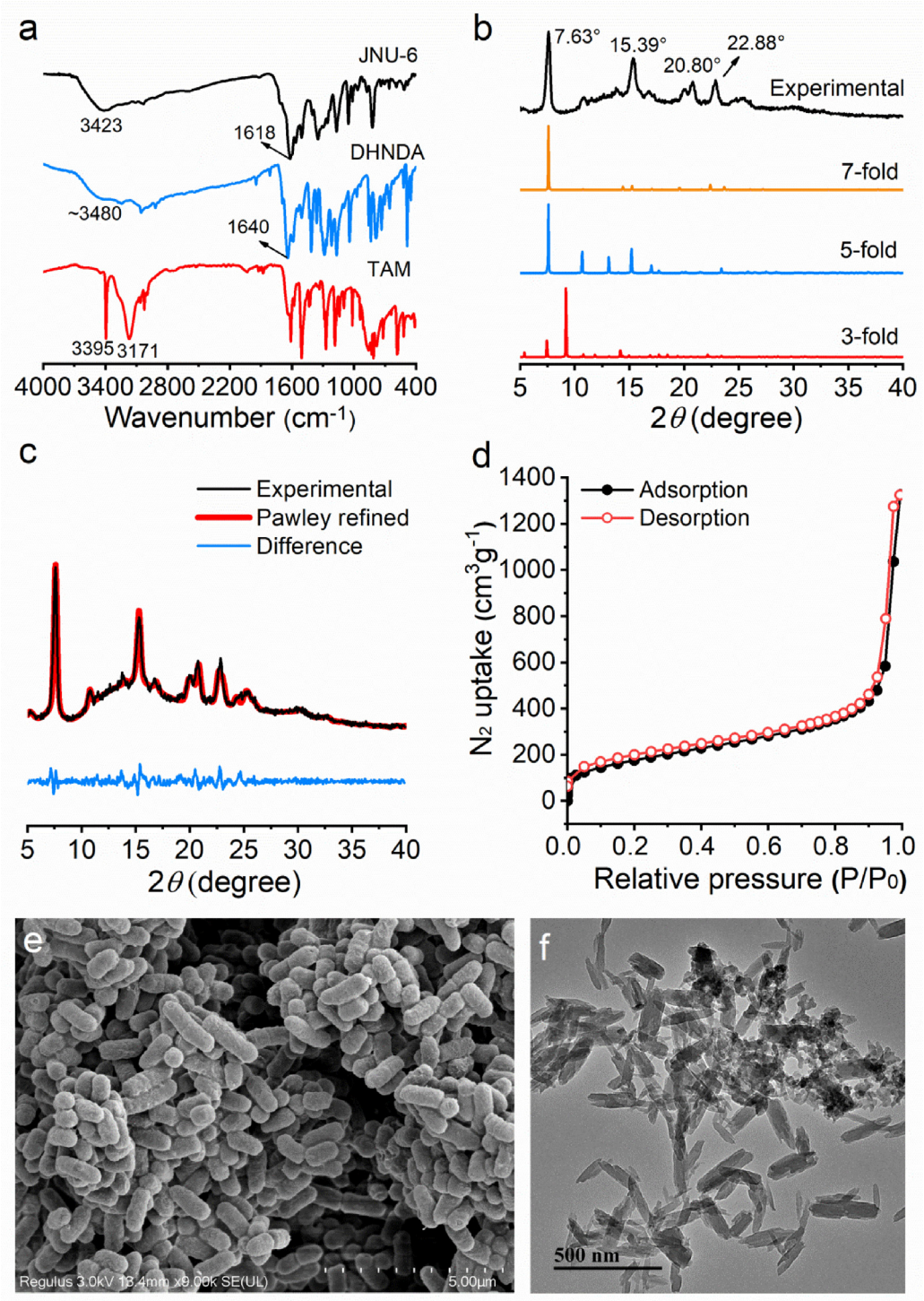

Fig. 2. (a) FTIR spectra of TAM (red), DHNDA (blue) and JNU-6 (black). (b) Comparison of PXRD patterns for JNU-6: experimental as well as calculated from the 3-fold, 5-fold and 7-fold interpenetrated dia nets. (c) Comparison of experimental and pawley refined PXRD patterns of JNU-6. (d) N_2 adsorption-desorption isotherms of JNU-6 (77 K). (e) SEM and (f) TEM images of JNU-6.

its (LODs) ($S/N = 3$) and quantification limits (LOQs) ($S/N = 10$) of the developed JNU-6 based DSPE-GC-FTD method for OPPs were in the range of 0.15–0.39 ng mL^{-1} and 0.58–1.50 ng mL^{-1}, respectively (Table 1). The relative standard deviations (RSD) of intraday ($n = 5$), interday ($n = 5$) and batch to batch ($n = 3$) for the determination of 100 ng mL^{-1} OPPs were in the ranges of 3.2%−5.7%, 4.4%−6.1% and 5.6%−7.3%, respectively. Furthermore, the retention of the PXRD pattern of JNU-6 after 5 cycles indicates the good reusability of JNU-6 (Figs. 5a and S12).

The comparison of the analytical performance between the JNU-6 based DSPE-GC-FTD and other adsorbents based analytical methods for OPPs is listed in Table S3. Our developed method gave lower LODs for OPPs in a shorter extraction time than most of the other adsorbent based methods, indicating the high potential of JNU-6 as adsorbent for the extraction of contaminant. Moreover, the extraction performance of recommended commercial adsorbent (Sep-PakNH_2) and the hydroxyl-free 3D COF (COF-300) was also investigated. For comparison, enhancement factors

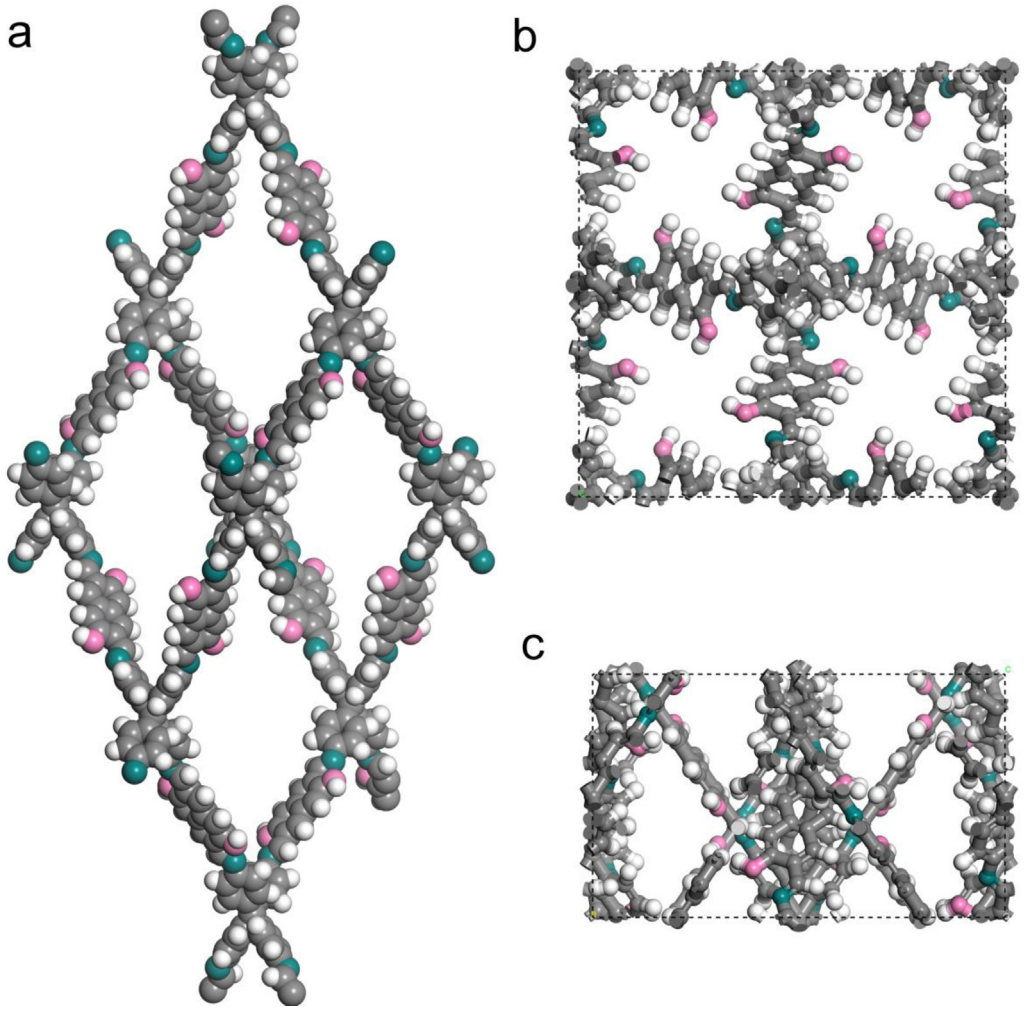

Fig. 3. (a) Structural representation of the unit of JNU-6. (b) Top view of JNU-6. (c) Side view of JNU-6. gray C, white H, green N, pink O.

Table 1
Analytical performance for the developed JNU-6 based DSPE-GC-FTD for the determination of OPPs.

Analytes	Linear range(ng mL^{-1})	R^2	LODs(ng mL^{-1})	LOQs(ng mL^{-1})	RSD(%)		
					Intraday ($n = 5$)	Interday ($n = 5$)	Batch-to-batch ($n = 3$)
PAM	1–1000	0.9981	0.20	0.77	4.5	5.8	7.2
PA	1–1000	0.9966	0.18	0.58	3.4	4.4	5.6
PFF	1–800	0.9968	0.15	0.67	3.2	4.9	6.3
PHO	3–1100	0.9997	0.39	1.50	5.7	6.1	7.3

(EFs) were determined as the ratio of the sensitivity of the analytes after extraction to that before extraction. The EFs of commercial Sep-PakNH_2 (2–4) was much lower than that of 3D COFs. Our hydroxyl-functionalized 3D COF JNU-6 gave much higher EF (17–80) than hydroxyl-free COF-300 (6–16), confirming the key role of hydroxyl for the extraction of OPPs (Fig. 5b). The excellent enrichment efficiency of JNU-6 for OPPs is greatly correlated to the structural and functional features of JNU-6. The large surface area of JNU-6 with rich porous channels allows the sufficient accessibility of OPPs and the active interaction sites [33]. The hydrophobic OPPs with aromatic ring can interact with JNU-6 via the hydrophobic interaction [34] and π-π interaction [35,36]. Moreover, the hydrogen bond between the N, O, S of OPPs and the hydroxyl of JNU-6 dominants the selective extraction of OPPs due to the lower EFs of hydroxyl-free COF-300 than JNU-6.

3.5. Method validation and analysis of real samples

A certified reference apple juice sample (MRM0666) was further applied to validate the developed method. The determined concentration of 0.090 ± 0.014 mg kg^{-1} for PFF agrees well with the certified value (0.085 ± 0.022 mg kg^{-1}). The developed method was also applied for the determination of OPPs in real samples of tomato, cabbage and apple. The analytical results are listed in Table 2. Only PA was found to be in the range of 1.33–2.14 μg kg^{-1} in the cabbage and tomato samples, while other OPPs were below the LODs or LOQs in all the studied samples. The recoveries of the OPPs in the real samples ranged from 85.6% to 106% with a precision of 1.6%–8.4% at three spike levels of 25, 50 and 100 μg kg^{-1} (Table 2). The representative extracted chromatograms of the OPPs in real samples are shown in Fig. S13.

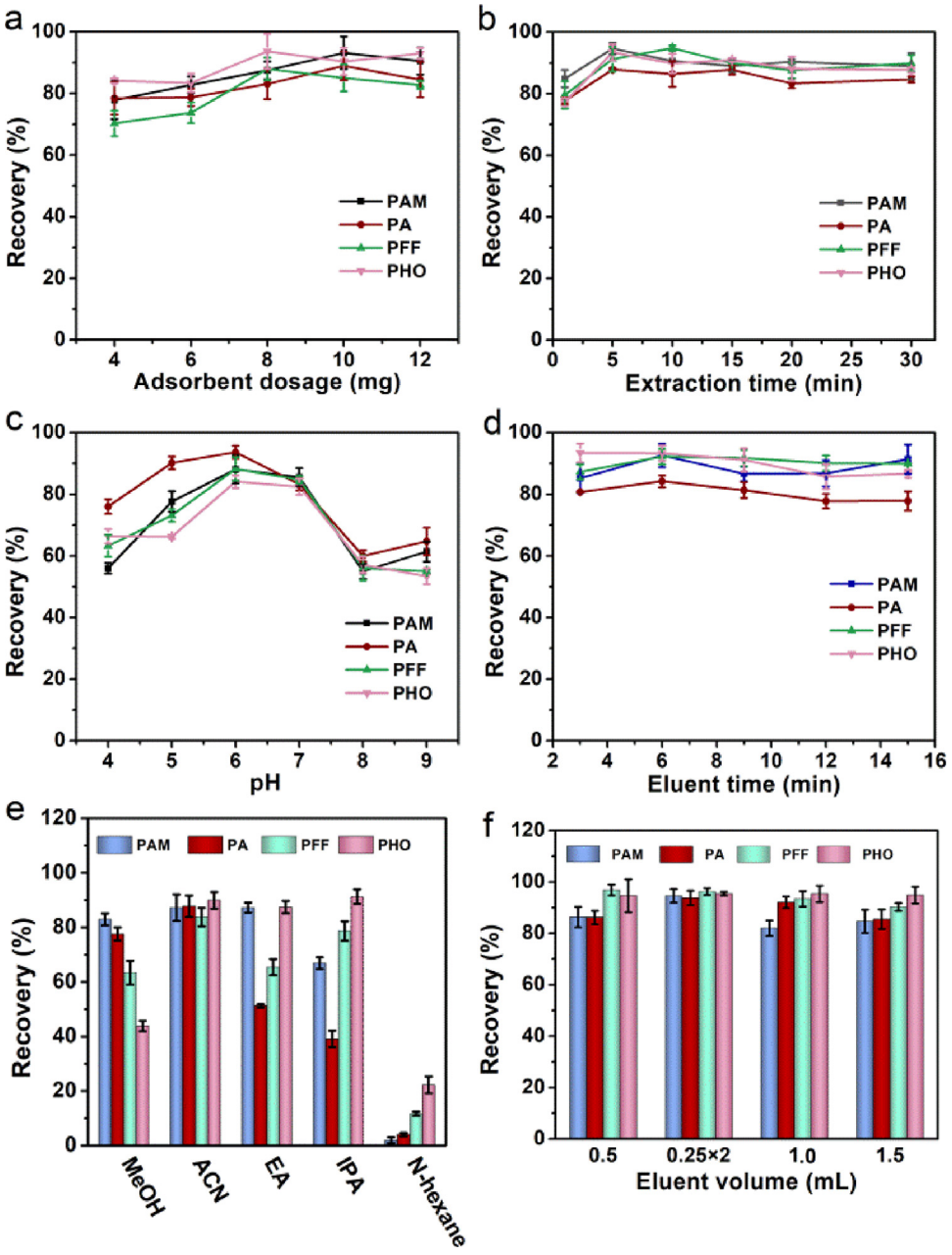

Fig. 4. Effect of experimental conditions: (a) amount of JNU-6, (b) extraction time, (c) pH, (d) elution time, (e) eluent and (f) eluent volume on the recovery of OPPs (40 ng mL^{-1}). Error bar represents one standard deviation for three replicate measurements.

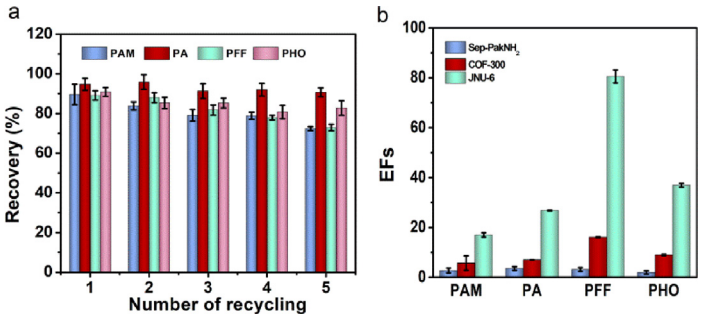

Fig. 5. (a) Reusability of JNU-6 for DSPE of OPPs (40 ng mL^{-1}). (b) DSPE enrichment factors of Sep-PakNH_2, COF-300 and JNU-6 for OPPs. Error bar represents one standard deviation for three replicate measurements.

Table 2
Analytical results for the determination of OPPs in fruit and vegetable.

Sample	Spiked(μg kg^{-1})	PAM		PA		PFF		PHO	
		Determined(μg kg^{-1})	Recovery (%)	Determined(μg kg^{-1})	Recovery (%)	Determined(μg kg^{-1})	Recovery (%)	Determined(μg kg^{-1})	Recovery (%)
Tomato	0.0	ND		1.33 ± 0.15		ND		ND	
	25.0	25.1 ± 2.2	100 ± 5	25.4 ± 0.9	96.4 ± 3.8	24.7 ± 1.0	98.8 ± 3.4	22.0 ± 5.5	87.9 ± 8.0
	50.0	48.2 ± 3.2	96.3 ± 4.8	52.3 ± 1.0	102 ± 3	52.5 ± 3.5	105 ± 7	46.9 ± 3.3	93.8 ± 5.3
	100.0	97.2 ± 4.5	97.2 ± 4.5	98.0 ± 2.0	98.0 ± 2.0	97.5 ± 3.1	97.5 ± 3.1	102 ± 4	102 ± 4
Cabbage	0.0	<LOQ		2.14 ± 0.07		ND		ND	
	25.0	23.8 ± 0.4	95.3 ± 1.6	24.8 ± 1.1	90.5 ± 3.4	23.2 ± 0.9	92.6 ± 2.6	25.5 ± 0.6	102 ± 2
	50.0	46.7 ± 1.0	93.3 ± 2.9	48.7 ± 1.0	93.0 ± 3.1	47.5 ± 2.6	95.0 ± 5.5	48.2 ± 1.0	96.4 ± 2.5
	100.0	90.3 ± 6.2	90.3 ± 6.2	101 ± 6	101 ± 6	94.9 ± 3.0	94.9 ± 3.0	95.7 ± 8.4	95.7 ± 8.4
Apple	0.0	<LOQ		<LOQ		<LOQ		ND	
	25.0	22.3 ± 2.1	89.2 ± 4.2	21.4 ± 1.2	85.6 ± 2.8	24.6 ± 1.1	98.3 ± 3.1	22.7 ± 2.4	90.8 ± 4.7
	50.0	51.5 ± 5.2	103 ± 7	49.3 ± 2.5	98.6 ± 5.6	47.1 ± 2.1	94.1 ± 5.0	50.6 ± 3.5	101 ± 6
	100.0	100 ± 8	100 ± 8	88.5 ± 4.1	88.5 ± 4.1	93.0 ± 8.4	93.0 ± 8.4	106 ± 4	106 ± 4

ND: Not detected. $n = 5$

4. Conclusion

In summary, we have reported the design and preparation of a novel hydroxyl-functionalized 3D COF JNU-6 with 5-fold interpenetrated diamond net via the condensation of symmetrical tetrahedral structure of TAM and linear planar structure of DHNDA. The high crystallinity, large surface area, good stability of the prepared JNU-6 with rich hydroxyl and aromatic ring endows JNU-6 with multi-interactions of hydrophobic interaction, hydrogen bonding interaction, and π-π interaction for rapid and selective extraction of OPPs. The developed JNU-6 based DSPE-GC-FTD method exhibits excellent analytical performance for the determination of OPPs in real samples. Our work reveals the high practical potential of functionalized 3D COFs as adsorbents for effective extraction of trace contaminants in complicated samples.

Declaration of Competing Interest

The authors declare no conflict of interest.

CRediT authorship contribution statement

Mei-Lan Du: Methodology, Data curation, Writing – original draft. **Cheng Yang:** Methodology. **Hai-Long Qian:** Conceptualization, Funding acquisition, Writing – review & editing. **Xiu-Ping Yan:** Funding acquisition, Resources, Supervision, Writing – review & editing.

Acknowledgments

This work was supported by the National Natural Science Foundation of China (22076066 and 22176073), the Fundamental Research Funds for the Central Universities (No. JUSRP221002), the Program of “Collaborative Innovation Center of Food Safety and Quality Control in Jiangsu Province”.

Supplementary materials

Supplementary material associated with this article can be found, in the online version, at doi:10.1016/j.chroma.2022.463071.

References

[1] W.A. Wattigney, E. Irvin-Barnwell, Z. Li, A. Ragin-Wilson, Biomonitoring of toxic metals, organochlorine pesticides, and polybrominated biphenyl 153 in Michigan urban anglers, Environ. Res. 203 (2022) 111851.
[2] G.D. Eudoxie, G. Mathurin, V. Lopez, O. Perminova, Assessment of pesticides in soil from obsolete pesticides stores: a Caribbean case study, Environ. Monit. Assess. 191 (2019) 498–507.
[3] L. Liu, X. Zheng, X. Wei, Z. Kai, Y. Xu, Excessive application of chemical fertilizer and organophosphorus pesticides induced total phosphorus loss from planting causing surface water eutrophication, Sci. Rep. 11 (2021) 23015.
[4] M. Syafrudin, R.A. Kristanti, A. Yuniarto, T. Hadibarata, J. Rhee, W.A. Al-Onazi, T.S. Algarni, A.H. Almarri, A.M. Al-Mohaimeed, Pesticides in drinking water-a review, Int. J. Environ. Res. Public Health 18 (2021) 468–483.
[5] Z. Li, J. Sun, L. Zhu, Organophosphorus pesticides in greenhouse and open-field soils across China: distribution characteristic, polluted pathway and health risk, Sci. Total Environ. 765 (2021) 142757.
[6] L.A. Pardo, L.E. Beane Freeman, C.C. Lerro, G. Andreotti, J.N. Hofmann, C.G. Parks, D.P. Sandler, J.H. Lubin, A. Blair, S. Koutros, Pesticide exposure and risk of aggressive prostate cancer among private pesticide applicators, Environ. Health 19 (2020) 30–42.
[7] J.R. Richardson, V. Fitsanakis, R.H.S. Westerink, A.G. Kanthasamy, Neurotoxicity of pesticides, Acta Neuropathol. 138 (2019) 343–362.
[8] P. Kuchheuser, M. Birringer, Evaluation of specific import provisions for food products from third countries based on an analysis of RASFF notifications on pesticide residues, Food Control 133 (2022) 108581.
[9] A. Tritscher, K. Miyagishima, C. Nishida, F. Branca, Ensuring food safety and nutrition security to protect consumer health: 50 years of the Codex Alimentarius commission, Bull World Health Organ. 91 (2013) 468 468A.
[10] European Commission, EU pesticides database. https://ec.europa.eu/food/plant/pesticides/eu-pesticides-database/mrls/?event=search.pr .

[11] J. da Silva Sousa, H.O. do Nascimento, H. de Oliveira Gomes, R.F. do Nascimento, Pesticide residues in groundwater and surface water: recent advances in solid-phase extraction and solid-phase microextraction sample preparation methods for multiclass analysis by gas chromatography-mass spectrometry, Microchem. J. 168 (2021) 106359.
[12] G.F. Pang, Y.M. Liu, C.L. Fan, J.J. Zhang, Y.Z. Cao, X.M. Li, Z.Y. Li, Y.P. Wu, T.T. Guo, Simultaneous determination of 405 pesticide residues in grain by accelerated solvent extraction then gas chromatography-mass spectrometry or liquid chromatography-tandem mass spectrometry, Anal. Bioanal. Chem. 384 (2006) 1366–1408.
[13] C. Yu, D. Hao, Q. Chu, T. Wang, S. Liu, T. Lan, F. Wang, C. Pan, A one adsorbent QuEChERS method coupled with LC-MS/MS for simultaneous determination of 10 organophosphorus pesticide residues in tea, Food Chem. 321 (2020) 126657.
[14] S.M. Khoshmanesh, H. Hamishehkar, H. Razmi, Trace analysis of organophosphorus pesticide residues in fruit juices and vegetables by an electrochemically fabricated solid-phase microextraction fiber coated with a layer-by-layer graphenized graphite/graphene oxide/polyaniline nanocomposite, Anal. Methods 12 (2020) 3268–3276.
[15] T. Boontongto, R. Burakham, Eco-friendly fabrication of a magnetic dual-template molecularly imprinted polymer for the selective enrichment of organophosphorus pesticides for fruits and vegetables, Anal. Chim. Acta 1186 (2021) 339128.
[16] P.G. Arias, H. Martínez-Pérez-Cejuela, A. Combès, V. Pichon, E. Pereira, J. Manuel Herrero-Martínez, M. Bravo, Selective solid-phase extraction of organophosphorus pesticides and their oxon-derivatives from water samples using molecularly imprinted polymer followed by high-performance liquid chromatography with UV detection, J. Chromatogr. A 1626 (2020) 461346.
[17] L. Liu, M. Yang, M. He, T. Liu, F. Chen, Y. Li, X. Feng, Y. Zhang, F. Zhang, Magnetic solid phase extraction sorbents using methyl-parathion and quinalphos dual-template imprinted polymers coupled with GC-MS for class-selective extraction of twelve organophosphorus pesticides, Microchim. Acta 187 (2020) 503–515.
[18] L. González, F.J. Carmona, N.M. Padial, J.A.R. Navarro, E. Barea, C.R. Mald onado, Dual removal and selective recovery of phosphate and an organophosphorus pesticide from water by a Zr-based metal-organic framework, Mater. Today Chem. 22 (2021) 100596.
[19] A. Jamali, F. Shemirani, A. Morsali, A comparative study of adsorption and removal of organophosphorus insecticides from aqueous solution by Zr-based MOFs, J. Ind. Eng. Chem. 80 (2019) 83–92.
[20] M. Wan, F. Xiang, Z. Liu, D. Guan, Y. Shao, L. Zheng, M. Jin, Y. She, L. Cao, F. Jin, R. Chen, S. Wang, Y. Wu, A.M. Abd El-Aty, J. Wang, Novel Fe_3O_4@metal-organic framework@polymer core-shell-shell nanospheres for fast extraction and specific preconcentration of nine organophosphorus pesticides from complex matrices, Food Chem. 365 (2021) 130485.
[21] Y. Liu, W. Li, C. Yuan, L. Jia, Y. Liu, A. Huang, Y. Cui, Two-dimensional fluorinated covalent organic frameworks with tunable hydrophobicity for ultrafast oil-water separation, Angew. Chem. Int. Ed. (2021) 61 e202113348.
[22] Q. Dang, H. Huang, L. Li, X. Lyu, S. Zhong, Y. Yu, D. Xu, Yolk–shell-structured covalent organic frameworks with encapsulated metal–organic frameworks for synergistic catalysis, Chem. Mater. 33 (2021) 5690–5699.
[23] J.Y. Yue, X.L. Ding, Y.T. Wang, Y.X. Wen, P. Yang, Y. Ma, B. Tang, Dual functional sp^2 carbon-conjugated covalent organic frameworks for fluorescence sensing and effective removal and recovery of Pd^{2+} ions, J. Mater. Chem. A 9 (2021) 26861–26866.
[24] R.A. Maia, F. Lopes Oliveira, V. Ritleng, Q. Wang, B. Louis, P. Mothe Esteves, CO_2 capture by hydroxylated azine-based covalent organic frameworks, Chem. Eur. J. 27 (2021) 8048–8055.
[25] S. Li, Q. Liang, S.A.H. Ahmed, J. Zhang, Simultaneous determination of five benzimidazoles in agricultural foods by core-shell magnetic covalent organic framework nanoparticle–based solid-phase extraction coupled with high-performance liquid chromatography, Food Anal. Method 13 (2020) 1111–1118.
[26] R.R. Liang, S.Q. Xu, L. Zhang, P. Chen, F.Z. Cui, Q.Y. Qi, J. Sun, X. Zhao, Rational design of crystalline two-dimensional frameworks with highly complicated topological structures, Nat. Commun. 10 (2019) 4609.
[27] Y.J. Hou, J. Deng, K. He, C. Chen, Y. Yang, Covalent organic frameworks-based solid-phase microextraction probe for rapid and ultrasensitive analysis of trace per- and polyfluoroalkyl substances using mass spectrometry, Anal. Chem. 92 (2020) 10213–10217.
[28] W.R. Cui, C.R. Zhang, R.H. Xu, X.R. Chen, R.H. Yan, W. Jiang, R.P. Liang, J.D. Qiu, High-Efficiency photoenhanced extraction of uranium from natural seawater by Olefin-Linked covalent organic frameworks, ACS EST Water 1 (2021) 440–448.
[29] X. Niu, W. Lv, Y. Sun, H. Dai, H. Chen, X. Chen, *In situ* fabrication of 3D COF-300 in a capillary for separation of aromatic compounds by open-tubular capillary electrochromatography, Mikrochim. Acta 187 (2020) 233–242.
[30] G. Lin, H. Ding, D. Yuan, B. Wang, C. Wang, A pyrene-based, fluorescent three-dimensional covalent organic framework, J. Am. Chem. Soc. 138 (2016) 3302–3305.
[31] S. Xu, C. Guo, Y. Li, Z. Yu, C. Wei, Y. Tang, Methyl parathion imprinted polymer nanoshell coated on the magnetic nanocore for selective recognition and fast adsorption and separation in soils, J. Hazard. Mater. 264 (2014) 34–41.
[32] X. Lin, X. Wang, J. Wang, Y. Yuan, S. Di, Z. Wang, H. Xu, H. Zhao, P. Qi, W. Ding, Facile synthesis of a core-shell structured magnetic covalent organic framework for enrichment of organophosphorus pesticides in fruits, Anal. Chim. Acta 1101 (2020) 65–73.
[33] N. Wang, Z. Liu, L. Wen, B. Zhang, C.A. Tao, J. Wang, Aptamer-binding zirconium-based metal-organic framework composites prepared by two conjunction approaches with enhanced bio-sensing for detecting isocarbophos, Talanta 236 (2022) 122822.
[34] S. He, T. Zeng, S. Wang, H. Niu, Y. Cai, Facile synthesis of magnetic covalent organic framework with three-dimensional bouquet-like structure for enhanced extraction of organic targets, ACS Appl. Mater. Interfaces 9 (2017) 2959–2965.
[35] Y. Jia, H. Su, Z. Wang, Y.E. Wong, X. Chen, M. Wang, T.D. Chan, Metal-organic framework@microporous organic network as adsorbent for solid-phase Microextraction, Anal. Chem. 88 (2016) 9364–9367.
[36] Q. Zhang, W. Xiao, Y. Wu, Y. Fan, W. Zou, K. Xu, Y. Yuan, X. Mao, Y. Wang, A simple, environmental-friendly and reliable d-SPE method using amino-containing metal-organic framework MIL-125-NH_2 to determine pesticide residues in pomelo samples from different localities, Food Chem. 372 (2022) 131208.